

## Molecular Kondo Chain

Andrew DiLullo,<sup>†,§</sup> Shih-Hsin Chang,<sup>†</sup> Nadjib Baadji,<sup>‡</sup> Kendal Clark,<sup>†,§</sup> Jan-Peter Klöckner,<sup>||</sup> Marc-Heinrich Prosenç,<sup>||</sup> Stefano Sanvito,<sup>‡</sup> Roland Wiesendanger,<sup>†</sup> Gernar Hoffmann,<sup>\*,†,⊥</sup> and Saw-Wai Hla<sup>\*,†,§</sup>

<sup>†</sup>Institute of Applied Physics, University of Hamburg, Germany

<sup>‡</sup>School of Physics and CRANN, Trinity College, Dublin 2, Ireland

<sup>§</sup>Nanoscale and Quantum Phenomena Institute, Department of Physics and Astronomy, Ohio University, Athens Ohio 45701, United States

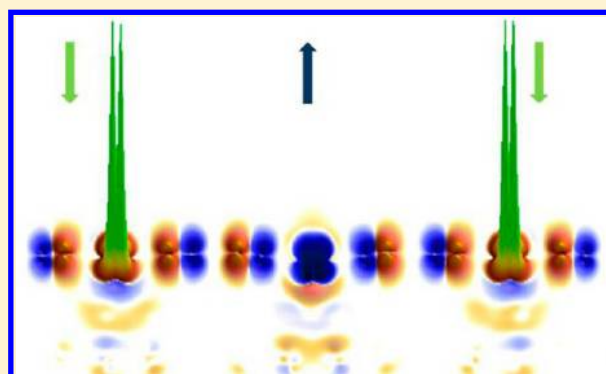
<sup>||</sup>Institute of Inorganic Chemistry, University of Hamburg, Germany

<sup>⊥</sup>Institute of Physics, Academia Sinica and Department of Physics, National Taiwan University, Taipei, Taiwan

### S Supporting Information

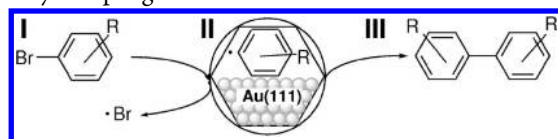
**ABSTRACT:** An important development in recent synthesis strategies is the formation of electronically coupled one and two-dimensional organic systems for potential applications in nanoscale molecule-based devices. Here, we assemble one-dimensional spin chains by covalently linking basic molecular building blocks on a Au(111) surface. Their structural properties are studied by scanning tunneling microscopy and the Kondo effect of the basic molecular blocks inside the chains is probed by scanning tunneling spectroscopy. Tunneling spectroscopic images reveal the existence of separate Kondo regions within the chains while density functional theory calculations unveil antiferromagnetic coupling between the spin centers.

**KEYWORDS:** Nanoscience and technology, scanning tunneling microscopy, spin chain, Kondo



Advances in spintronic applications such as data storage and quantum computation rely on the ability to tailor magnetic transport and spin properties of nanostructures.<sup>1–3</sup> Recently, great progress in the study of spin-related properties on single molecules by local probes has been achieved.<sup>4–14</sup> Independently, synthetic routines on controlled polymerization into one-dimensional molecular wires and two-dimensional molecular networks have been developed for molecular electronics.<sup>15–18</sup> Here, we combine both approaches and create molecular chains containing multiple spins on a metal surface by polymerization of the ligand structure. Our approach constitutes a significant step forward because, due to their large sizes, multi-spincenter macromolecules are difficult to thermally deposit intact.<sup>19</sup> As such the scheme presented here appears as a viable strategy for making larger molecules containing a network of spins compatible with ultrahigh-vacuum processing.

The molecular chains containing multiple spin centers are assembled from basic molecular blocks using surface catalyzed aryl–aryl coupling reactions<sup>15,20–22</sup>



Here, when thermally activated, Br–aryl bonds (I) are broken and intermediate reactants are formed (II), which then join to create biaryls (III).<sup>20–22</sup> During the reaction process, the Au substrate acts as a catalyst. In the reaction schematic presented above, R represents any metal–organic fragment, which in this case is host to a magnetic Co atom. We chose Co(*S,S'*-Br<sub>2</sub>-Salophen) (Figure 1a,b), a salen type complex,<sup>23,24</sup> to act as the basic building blocks of the molecular chains after debromination. In this molecule, the Co<sup>II</sup> ion is square-planar tetra coordinated and possesses a low spin d<sup>7</sup> electron configuration exhibiting one unpaired electron (*S* = 1/2), and the two opposing arms of the molecules are functionalized with bromine for coupling reactions.<sup>15,20–22</sup> The molecules were thermally deposited onto an atomically clean Au(111) surface held at room temperature under ultrahigh vacuum. The molecules form well-ordered clusters on Au(111) (Figure 1c) mediated by weak intermolecular dipolar interactions at the halogen terminations<sup>23</sup> (Figure 1d). However, there is no direct chemical linking between individual molecules. Measurements were performed by using a custom-built scanning tunneling

Received: March 25, 2012

Revised: April 15, 2012

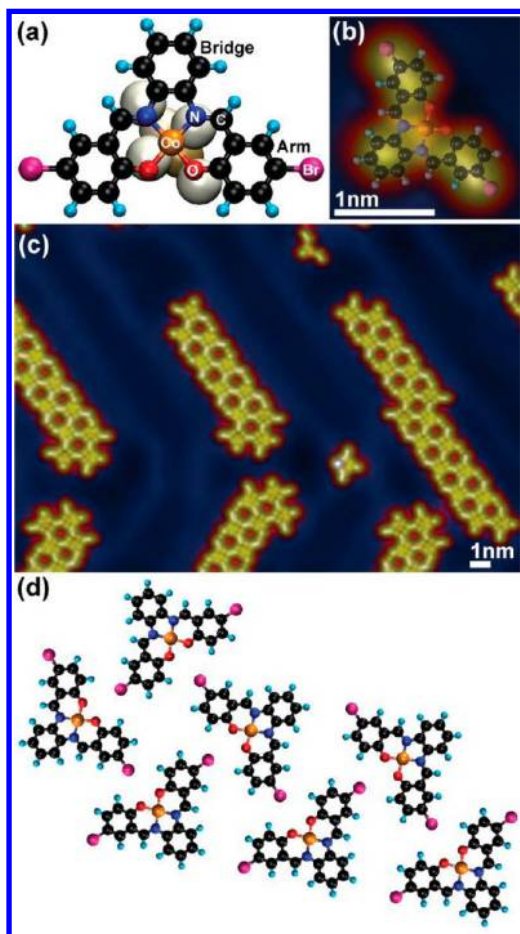


**Figure 1.** Co-(5,5'-Br<sub>2</sub>-Salophen) on Au(111) in (a) a structure model after relaxation on Au(111) and (b) as recorded in the experiment. (c) Self-assembled clusters on Au(111) ( $U = -200$  mV,  $I = 141$  pA) and (d) an illustration of the relative alignment of molecules as deduced from the experiment.

microscope (STM) system at 6 K. The tunneling spectroscopy data were measured by lock-in amplification using 2–5 mV rms modulation (650–1350 Hz).

Formation of magnetic molecular chains requires covalent linking between the end phenyl groups of the basic blocks after Br removal. This is realized by raising the Au(111) substrate temperature to 400 K for 10 min. During this process, a thermally activated Au-catalyzed aryl–aryl coupling reaction I→III occurs. After annealing, molecular chains primarily composed of basic blocks are found on the surface (Figure 2a), and molecular clusters formed by individual molecules are no longer present. Within chains, the central phenyl-bridge of the basic blocks can be positioned either parallel or antiparallel to each other. The molecular structure without the bromine substituents can be fit into the basic blocks of the chain (Figure 2b) and the distance between adjacent Co centers is approximately equal to the expected length of the debrominated molecules indicating a covalent linking between the basic blocks.<sup>25</sup> Covalent linking was further confirmed by STM lateral manipulation<sup>26</sup> (Figure 2c,d) where the joined molecular chains are observed to move as fixed units indicating rigid intrachain binding.

To understand the properties of engineered molecular chains on the surface, density functional theory (DFT) calculations are performed with the localized pseudoatomic-orbital basis and

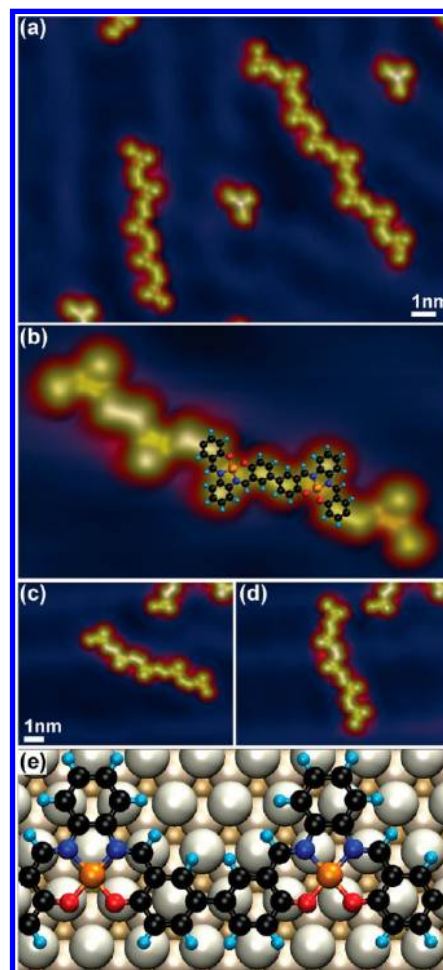


**Figure 2.** Molecular chains. (a) Overview image of magnetic molecular chains on Au(111) ( $U = 50$  mV,  $I = 300$  pA). Close up image of a 5-block molecular chain (b) with the chemical structure superimposed over the initial image. The molecular chain is laterally manipulated with the STM tip from (c) to (d), and it remains intact ( $U = 200$  mV,  $I = 1000$  pA; manipulation parameters:  $U = 200$  mV,  $I = 200$  nA,  $v = 11$  nm/s). (e) Calculated molecular chain structure on Au(111).

pseudopotential code SIESTA.<sup>27</sup> A user optimized basis set of double- $\zeta$  quality is used to describe all the valence atomic orbitals except for O-2p, N-2p, Br-4p, and Co-4p where additional polarized orbitals are included. For the gold substrate, an optimized single  $\zeta$  for 6s, 6p, and 5d is used to calculate the relaxed structure and only the 6s orbitals described with an optimized single  $\zeta$  is considered in the calculations. The core electrons for each atomic species are described by norm-conserving Troullier–Martin pseudopotentials<sup>28</sup> with nonlinear core correction.<sup>29</sup> The generalized gradient approximation with the standard Perdew–Burke–Ernzerhof (PBE) parametrization<sup>30</sup> is used to describe the exchange–correlation potential. The DFT calculations show a relatively large distance (2.9 to 3.1 Å) between the molecular chains and Au(111), so that the chains are either weakly chemisorbed or physisorbed. Calculations also reveal that the basic blocks in the chains remain in the planar geometry (Figure 2e), and there is no significant hybridization with the surface, that is, no chemical bond between the chains and the surface. Moreover, the ionization potential is found to decrease in absolute value with length while the electron affinity increases (it becomes more positive). This is due to the electronic coupling between the

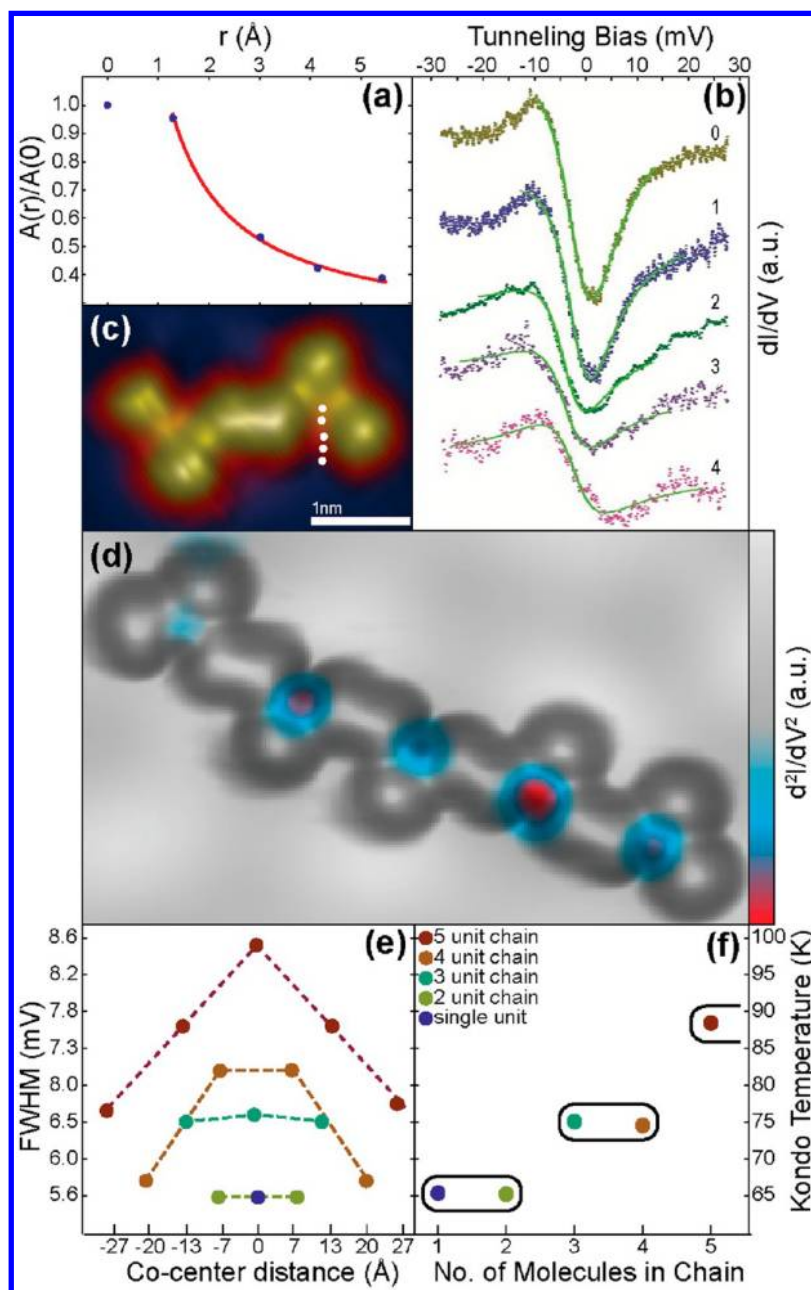


**Figure 3.** Kondo resonance. (a) The plot of Kondo amplitudes corresponding to (b) as a function of distance. (b) The distance dependence of the Fano amplitude observed on the locations indicated as 0, 1, 2, 3, and 4 in (a). (c) STM image of a two-block Kondo chain. (d) A color-encoded spectroscopic map overlaid with the simultaneously acquired STM image, [ $U = -5$  mV,  $I = 500$  pA,  $\Delta U = 3$  mV,  $f = 1333$  Hz]. (e) Chain length dependent energy and  $T_K$  (average data over multiple chains)<sup>42</sup> as measured from the middle of the chain. (f)  $T_K$  as averaged of entire chains with an observable even-odd asymmetry.

molecules, which splits the highest occupied molecular orbital (HOMO) and lowest unoccupied molecular orbital (LUMO) in multiplets with bonding and antibonding components. Since the spin-polarized HOMO is completely filled, the outermost single particle level of a molecule made by fusing two or more salophens has antibonding nature, that is, it is higher in energy with respect to the HOMO of the single molecule. Likewise, since the LUMO is empty, the lowermost unoccupied state has a bonding nature and it is lower than the LUMO of the single molecule. Such increase in the ionization energy and the decrease in the electron affinity have also been demonstrated in chain type molecules like polyC-polyG A-DNA strands<sup>31</sup> as well as in polyacetylene, poly p-phenylene, polythiophene, and

polypyrrole systems.<sup>32</sup> As a consequence, when the chain gets longer it is easier to accommodate the extra charge. This mechanism weakens the molecule-surface (C–Au) interaction.

Each basic block in the chains has an unpaired electron at the central Co atom. Calculations reveal that the net spin is still preserved in the basic blocks after covalent linking. If there is a nonzero net spin, many body interactions between the localized spin and free electrons from the surface can occur, resulting in what is commonly called the Kondo effect. This effect may be observed in  $dI/dV - V$  spectroscopic measurements as a Fano line-shape feature near the Fermi level.<sup>5–9,33</sup> The specific shape reflects the competition between tunneling electrons directly interacting with the localized spin and tunneling electrons

indirectly interacting with the localized spin through the spin-correlated surface electrons. The shape of this spectroscopic feature depends strongly on the substrate–adsorbate coupling strength and so is largely system dependent.

A Kondo resonance state is clearly observed when  $dI/dV - V$  spectra are recorded above the Co atom locations in the chains. The observed Kondo resonances are fitted by Fano line shapes using the relation:<sup>34</sup>

$$\frac{dI}{dV} = a(r) \frac{q(r)^2 + 2q(r)\varepsilon + 1}{1 + \varepsilon^2} + \text{const},$$

$$\varepsilon = \frac{meV + \Delta E}{k_B T_K}, \quad \text{and} \quad A(r) = a(r)[1 + q(r)^2]$$

Here,  $q(r)$  is the asymmetry parameter,  $k_B$  the Boltzmann constant,  $\Delta E$  the energy shift from  $E_F$ , and  $A(r)$  is the Kondo amplitude. The energy width of the resonance quantifies the spin-electron interaction strength in terms of the Kondo temperature,  $T_K$ . To further confirm that the feature observed in spectroscopic measurements is due to the Kondo effect we have taken spectra along a path from the Co ion site to the clean Au(111) surface as shown in Figure 3c. These spectra, reproduced in Figure 3b, were fit with the Fano equation to extract  $A(r)$ . The Kondo amplitudes are plotted as a function of the distance from the Co site (Figure 3a), and are observed to closely follow the  $1/r$  (where  $r$  is the distance from the localized spin) behavior while the extracted Kondo temperatures remain constant, as can be expected for Kondo systems.<sup>35</sup>

In order to gain further insight into the spatial extent of the Kondo resonance, often  $dI/dV$  maps are used to image the local density of states (LDOS).<sup>33</sup> Here, we directly probe the more sensitive second derivative ( $d^2I/dV^2$ ) signal acquired at the energy of largest change in the LDOS.<sup>36</sup> In Figure 3d, the second derivative map is overlaid onto a three-dimensional representation of the simultaneously acquired surface topography. As observed in Figure 3d, the Kondo active sites are localized at the Co atoms, and so we have created covalently bound chains (macromolecules) with multiple spin-interaction sites from basic molecular units. While the spatial locations of the Kondo regions are identified via the spectroscopic maps, the energy widths of the Kondo resonances have to be determined by varying bias and therefore the  $dI/dV - V$  spectroscopy is a suitable scheme. Interestingly, we find the Kondo resonance widths, and the corresponding  $T_K$  values are dependent on the number of basic blocks in the molecular chains (Figure 3e,f) for up to five unit chains that we can form in the current work. The significant change in  $T_K$  values is indicative for a magnetic interaction among the spin centers. The average  $T_K$  increases with increasing chain length and is also dependent on the even or odd number of molecular units within the chains. Such an even–odd asymmetry suggests an antiferromagnetic (AFM) coupling and as in the ferromagnetic (FM) case the total spin would linearly increase with the number of Co centers.

To understand the observed effect, we performed spin resolved DFT calculations. In general, the Co-d orbital in planar square geometry splits in a doublet ( $xz, yz$ ) and three singlets. Because of the coordination to oxygen and nitrogen atoms, the symmetry is reduced and the doublet splits further into two singlets ( $xz, yz$ ). Therefore, the Co atom has a low spin state ( $S = 1/2$ ) with three occupied and one partially occupied singlets. Because of the planar structure and respectively, a stronger  $p\pi-d\pi$  ( $\pi$ ) overlapping than a  $p\sigma-d\sigma$

( $\sigma$ ), the exchange splitting in  $d_{xz}$  of  $\Delta_{ex} \sim 1.2$  eV is larger than that of the  $d_z^2$  which accounts for  $\sim 0.6$  eV. Thus, the  $d_z^2$  is the HOMO and  $d_{xz}$  is the LUMO (Figure 4a). In this electronic

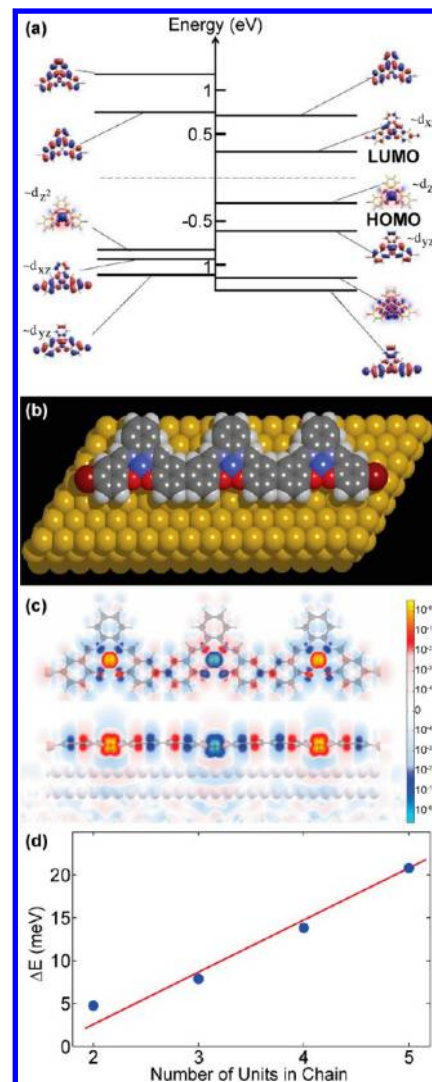


**Figure 4.** Theoretical electronic structure. (a) Molecular orbitals with their associated characters. (b) The 3-block molecular chain on Au(111) slab used in calculation. (c) Spin-up and down density distribution (blue and red color plots) within molecular chain; top view (top) and side view (bottom). (d)  $\Delta E$  versus the number of blocks in the molecular chain.

configuration, the partially unoccupied singlet is a  $d_{xz}$  and it carries the spin of the Co atom. After the removal of the Br atom, the last C atom of a basic unit remains with an unpaired electron that is FM coupled to the localized  $d_{xz}$  electron of the Co at the center. Respectively, an antiferromagnetic linker unit is created during the chain formation when two of such electrons pair into a singlet state and form a new covalent C–C bond (Figure 4b). Calculations reveal that the spin densities of the Co centers inside the chains are localized (Figure 4c) in accordance with the acquired Kondo map (Figure 3d). Thus, a possible reason for such even/odd number dependence in  $T_K$  might be due to an AFM coupling between the spin-centers. Indeed, Tsukahara et al.<sup>37</sup> reported the coexistence of Kondo with AFM in molecular clusters where the coupling is through a long-range surface mediated RKKY interaction<sup>38–40</sup> and has

been observed for the Kondo widths below 2 meV. In our case, comparison between the calculated results of the magnetic interactions inside a molecular chain in vacuum and that on the substrate shows no significant change in the AFM coupling strength but only a low spin-density induced into the Au surface compared to the spin-density residing on the organic ligand. AFM and FM couplings in the chains increase with the increasing number of Co centers. Figure 4d shows a plot of  $\Delta E$  as a function of molecular units for molecular chains in vacuum. This leads us to conclude that the interaction between the Co atoms in the chains is within the molecule and that the substrate has little effect for the molecule-surface distance range ( $\sim 3 \text{ \AA}$ ) considered here.

In summary, our experimental observations demonstrate the first successful on-surface creation of multispin center macro-molecules. DFT calculations and spectroscopic measurements reveal that the molecular spins are magnetically coupled and remain localized on the Co centers. More importantly, the basic units are linked via covalent bonding, which might maintain magnetic coupling for higher temperatures than dipolar and van der Waals interactions in conventionally self-assembled structures, which are only suitable up to a few Kelvin. Extending this approach with heteromolecular catalysis and design of multifunctional spin systems<sup>41</sup> may enable bottom up engineering of molecular and hybrid-molecular nanospinronic structures for future applications.

## ■ ASSOCIATED CONTENT

### Supporting Information

Additional information and figure. This material is available free of charge via the Internet at <http://pubs.acs.org>.

## ■ AUTHOR INFORMATION

### Notes

The authors declare no competing financial interest.

## ■ ACKNOWLEDGMENTS

We acknowledge useful discussions with S. E. Ulloa and experimental support by J. Brede and S. Kuck. This work is financially supported by the NSF PIRE, OISE 0730257, DFG (SFB 668-A4, A5 and GrK 611), the EU project SpiDME, SFI (08/ERA/I1759), and the Hamburg Cluster of Excellence NANOSPINTRONICS.

## ■ REFERENCES

- (1) Wegner, D.; Yamachika, R.; Zhang, X.; Wang, Y.; Baruah, T.; Pederson, M. R.; Bartlett, B. M.; Long, J. R.; Crommie, M. F. *Phys. Rev. Lett.* **2009**, *103*, 087205–4.
- (2) Park, J.; Pasupathy, A. N.; Goldsmith, J. I.; Chang, C.; Yaish, Y.; Petta, J. R.; Rinkoski, M.; Sethna, J. P.; Abruna, H. D.; McEuen, P. L.; Ralph, D. C. *Nature* **2002**, *417*, 722–725.
- (3) Atodiresei, N.; Caciuc, V.; Lazic, P.; Blügel, S. *Phys. Rev. B* **2011**, *84*, 172402.
- (4) Liang, W.; Shores, M. P.; Bockrath, M.; Long, J. R.; Park, H. *Nature* **2002**, *417*, 725–729.
- (5) Franke, K. J.; Schulze, G.; Pascual, J. I. *Science* **2010**, *332*, 940–944.
- (6) Chiappe, G.; Louis, E. *Phys. Rev. Lett.* **2006**, *97*, 076806.
- (7) Zhao, A.; Li, Q.; Chen, L.; Xiang, H.; Wang, W.; Pan, S.; Wang, B.; Xiao, X.; Yang, J.; Hou, J. G.; Zhu, Q. *Science* **2005**, *309*, 1542–1544.
- (8) Fu, Y.-S.; Ji, S.-H.; Chen, X.; Ma, X.-C.; Wu, R.; Wang, C.-C.; Duan, W.-H.; Qiu, X.-H.; Sun, B.; Zhang, P.; Jia, J.-F.; Xue, Q.-K. *Phys. Rev. Lett.* **2007**, *99*, 256601.
- (9) Iancu, V.; Deshpande, A.; Hla, S.-W. *Phys. Rev. Lett.* **2006**, *97*, 266603.
- (10) Brede, J.; Atodiresei, N.; Kuck, S.; Lazic, P.; Caciuc, V.; Morikawa, Y.; Hoffmann, G.; Blügel, S.; Wiesendanger, R. *Phys. Rev. Lett.* **2010**, *105*, 047204.
- (11) Atodiresei, N.; Brede, J.; Lazic, P.; Caciuc, V.; Hoffmann, G.; Wiesendanger, R.; Blügel, S. *Phys. Rev. Lett.* **2010**, *105*, 066601.
- (12) Komeda, T.; Isshiki, H.; Liu, J.; Zhang, Y.-F.; Lorente, N.; Katoh, K.; Breedlove, B. K.; Yamashita, M. *Nat. Commun.* **2011**, *2*, 217.
- (13) Lodi Rizzini, A.; Krull, C.; Balashov, T.; Kavich, J. J.; Mugarza, A.; Miedema, P. S.; Thakur, P. K.; Sessi, V.; Klyatskaya, S.; Ruben, M.; Stepanow, S.; Gambardella, P. *Phys. Rev. Lett.* **2011**, *107*, 177205.
- (14) Mannini, M.; Pineider, F.; Danieli, C.; Totti, F.; Sorace, L.; Sainctavit, P.; Arrio, M.-A.; Otero, E.; Joly, L.; Cezar, J. C.; Cornia, A.; Sessoli, R. *Nature* **2010**, *468*, 417–421.
- (15) Grill, L.; Dyer, M.; Lafferentz, L.; Persson, M.; Peters, M. V.; Hecht, S. *Nat. Nanotechnol.* **2007**, *2*, 687.
- (16) Barth, J. V. *Surf. Sci.* **2009**, *603*, 1533–1541.
- (17) Kittelmann, M.; Rahe, P.; Nimmrich, M.; Hauke, C. M.; Gourdon, A.; Kühnle, A. *ACS Nano* **2011**, *5*, 8420.
- (18) Abel, M.; Clair, S.; Ourdjini, O.; Mossoyan, M.; Porte, L. *J. Am. Chem. Soc.* **2011**, *133*, 1203–1205.
- (19) Sanvito, S. *Chem. Soc. Rev.* **2011**, *40*, 3336–3355.
- (20) Blake, M. M.; Nanayakkara, S. U.; Claridge, S. A.; Fernández-Torres, L. C.; Sykes, E. C. H.; Weiss, P. S. *J. Phys. Chem. A* **2009**, *113*, 13167–13172.
- (21) Hla, S.; Bartels, L.; Meyer, G.; Rieder, K. *Phys. Rev. Lett.* **2000**, *85*, 2777–2780.
- (22) Ullmann, F.; Bielecki, J. *Chem. Ber.* **1901**, *34*, 2174.
- (23) Kuck, S.; Chang, S.-H.; Klöckner, J.-P.; Prosenic, M. H.; Hoffmann, G.; Wiesendanger, R. *ChemPhysChem* **2009**, *10*, 2008–2011.
- (24) Badjib, N.; Kuck, S.; Brede, J.; Hoffmann, G.; Wiesendanger, R.; Sanvito, S. *Phys. Rev. B* **2010**, *82*, 115447.
- (25) We note that on Cu(111) chain formation can also be observed but an additional topographical feature appears at the intersection and chains are additionally elongated. Although not further investigated and in agreement with Grill et al., *J. Am. Chem. Soc.* **2010**, *132*, 16848, this can be interpreted as a formation of a molecule-Cu-molecule structure. This is not observed on Au(111) and therefore excluded for the present case.
- (26) Hla, S.-W. *J. Vac. Sci. Technol. B* **2005**, *23*, 1351–1360.
- (27) Soler, J. M.; Artacho, E.; Gale, J. D.; Gracia, A.; Junquera, J.; Ordejon, P.; Sanchez-Porta, D. *J. Phys.: Condens. Matter* **2002**, *14*, 2745.
- (28) Troullier, N.; Martins, J. L. *Phys. Rev. B* **1991**, *43*, 8861–8869.
- (29) Zhu, J.; Wang, X. W.; Louie, S. G. *Phys. Rev. B* **1992**, *45*, 8887–8893.
- (30) Perdew, J. P.; Burke, K.; Ernzerhof, M. *Phys. Rev. Lett.* **1996**, *77*, 3865–3868.
- (31) Pemmaraju, C. D.; Rungger, I.; Chen, X.; Rocha, A. R.; Sanvito, S. *Phys. Rev. B* **2010**, *82*, 125426.
- (32) Bredas, J. L.; Silbey, R.; Boudreaux, D. S.; Chance, R. R. *J. Am. Chem. Soc.* **1983**, *105*, 6555.
- (33) Perera, U. G. E.; Kulik, H. J.; Iancu, V.; Dias da Silva, L. G. G. V.; Ulloa, S. E.; Marzari, N.; Hla, S.-W. *Phys. Rev. Lett.* **2010**, *105*, 106601.
- (34) Ujsaghy, O.; Kroha, J.; Szunyogh, L.; Zawadowski, A. *Phys. Rev. Lett.* **2000**, *85*, 2557–2560.
- (35) Knorr, N.; Schneider, M. A.; Diekhöner, L.; Wahl, P.; Kern, K. *Phys. Rev. Lett.* **2002**, *88*, 096804.
- (36) Jiang, Y.; Zhang, Y. N.; Cao, J. X.; Wu, R. Q.; Ho, W. *Science* **2011**, *324*, 333.
- (37) Tsukahara, N.; Shiraki, S.; Itou, S.; Ohta, N.; Takagi, N.; Kawai, M. *Phys. Rev. Lett.* **2011**, *106*, 187201.
- (38) Ruderman, M. A.; Kittel, C. *Phys. Rev.* **1954**, *96*, 99–102.
- (39) Kasuya, T. *Prog. Theor. Phys.* **1956**, *16*, 45–57.
- (40) Yosida, K. *Phys.* **1957**, *106*, 893–898.

(41) Tanifuji, N.; Irie, M.; Matsuda, K. *J. Am. Chem. Soc.* **2005**, *127*, 13344–13353.

(42) For completeness, Figure 3e,f also includes the respective values as recorded on single molecules before chain formation that shows no significant variation ( $\Delta E < 0.5$  meV) between isolated and agglomerated molecules. This is a further indication that surface-mediated interaction is comparably weak.